Hydrogen evolution and pollutant purification over $NiMoO_4$/Twinned $Mn_{0.5}Cd_{0.5}S$ mediated by ·OH radicals in alkaline media

Zhuonan Lei [a], Wenhua Xue [b], Haijiao Xie [c], Tao Sun [a], Enzhou Liu [a,*]

[a] School of Chemical Engineering/Shaanxi Key Laboratory for Carbon Neutral Technology, Northwest University, Xi'an 710069, P. R. China

[b] Research Center for Eco-Environmental Engineering, Dongguan University of Technology, Dongguan, Guangdong 523808, China

[c] Hangzhou Yanqu Information Technology Co., Ltd., Hangzhou 310003, China

Email address: liuenzhou@nwu.edu.cn (Enzhou Liu)

1 Experimental sections

1.1 Preparation of twin $Mn_{0.5}Cd_{0.5}S$ solid solution nanoparticles (T-MCS)

T-MCS nanoparticles were synthesized via a solvothermal synthesis process as described below (**Fig**. 1a): Specifically, 1 mmol of $Cd(Ac)_2·4H_2O$ and an equivalent amount of $Mn(Ac)_2·4H_2O$ were dissolved in 60 mL of water under continuous stirring to ensure thorough mixing. Subsequently, the pH of the solution was gradually adjusted to approximately 13 by adding NaOH over a period of 30 min. Thereafter, 4 mmol of TAA was introduced into the solution, which was then transferred to a high-pressure autoclave for solvothermal treatment at 180° C for 18h. Upon cooling, the bright yellow precipitate was centrifuged and washed repeatedly with ethanol and water, and dried overnight at 60 °C. For comparison, WZ-MCS nanoparticles were synthesized by substituting 4 mmol of TAA with 2 mmol of L-cysteine, while ZB-MCS nanoparticles were produced using a similar method but with increased amounts of Mn and Cd precursors without adjusting the pH.

1.2 Materials

Manganese(ii) acetate tetrabydrate ($Mn(Ac)_2·4H_2O$) and Chromium acetate tetrahydrate ($Cd(Ac)_2·4H_2O$) was purchased from Tianjin Guangfu Fine Chemical Research Institute.

Thioacetamide (C_2H_5NS) was received from Shanghai Macklin Biochemical Technology Co., Ltd. sodium hydroxide (NaOH) and L-cysteine were purchased from Damao Chemical Reagent factory. $Na_2MoO_4 \cdot 2H_2O$ were purchased from Sinopharm Group Chemical Reagent Co., Ltd. $NiCl_2 \cdot 6H_2O$ Tianjin Comio Chemical Reagent Co., Ltd.

2 Physic characterization

X-ray diffraction (XRD, Rigaku Smart LAB SE) was used to obtain crystalline phase of the samples. The elemental composition, chemical state and morphology of the samples were characterized by X-ray photoelectron spectroscopy (XPS, Kratos AXIS NOVA), scanning electron microscope (SEM, Carl Zeiss SIGMA) equipped with an energy dispersive spectrometer (EDS). Transmission Electron Microscope (TEM, FEI Talos F200x) was also used to observe the morphology of the samples under 200kV. UV-vis diffuse reflection spectrophotometry (UV-vis DRS, Shimadzu UV-3600) was performed to analyze the light absorption properties of the catalysts. The photoluminescence spectra were measured by a florescence spectrophotometer (PL, Hitachi F7000). Time-resolved transient photoluminescence spectra (TRPL, Edinburgh FLS1000). Electron Paramagnetic Resonance (EPR, Bruker EMXplus-6/1) was used to study the free radicals of the samples. Zeta potential was characterized by Zetasizer Ultra (Malvern Zetasizer Nano ZS90). Optical Contact Angle (KINO, SL200KB) was used to test the contact angle of catalysts. In-situ irradiated X-ray Photoelectron Spectroscopy (ISI-XPS, ULVAC PHI5000) was characterized the chemical state and morphology of the samples.

3 Photochemical test

The photoelectric test of the samples was evaluated on an electrochemical workstation (CHI660E, ChenHua in Shanghai) with a standard three-electrode system in 0.1 M Na_2SO_4 electrolyte (pH=7).

Among them, a platinum wire and a standard calomel electrode (SCE) are used as the counter electrode and the reference electrode, respectively. The working electrode is prepared as follows: 3 mg of samples was dispersed in 3 mL of deionized water and 50 μL 1 *wt.*% naphthol, after ultrasonic treatment 2 h. 1 mL of homogeneous solution was dropped on 2 cm×3 cm FTO glass and dried at room temperature naturally. The transient photocurrent response (I-t curve, at 0.5 V potential *vs*. SCE), electrochemical impedance spectroscopy (EIS, frequency ranging from 10^{-2} to 10^{5} Hz), MS (Mott–Schottky curves, ranging from -1.2 V to 0 V *vs*. SCE), LSV curve analysis (linear sweep voltammetry curves, ranging from 0 to 1.6 V *vs*. SCE), multi-potential steps I-t plots (ranging from 0.2 to 0.5 V *vs*. SCE) and CV (cyclic voltammetry curve, ranging from 0.2 to 0.4 V *vs*. SCE) were measured in this work.

4 Photocatalytic H_2 evolution experiment

Photocatalytic H_2 evolution was conducted in a quartz Pyrex glass reactor (Lab-solar III-AG, Beijing Perfect Light Technology Co. Ltd, China). The experimental procedure was as follows: 10 mg of catalyst was dispersed in 100 mL various NaOH solutions under continuous stirring, which was then exposed to a 300 W Xe-lamp. Meanwhile, the external jacket of the reactor was connected to circulating water for precise temperature control during the reaction. Prior to light irradiation, the system underwent vacuum treatment to eliminate air contaminants. The amount of H_2 produced every 30 min was determined using an online GC7900 gas chromatograph equipped with N_2 as the carrier gas at a flow rate of 30 mL/min. The temperatures of the injector, chromatographic column and thermal conductivity detector were 80 ℃, 100 ℃ and 120 ℃, respectively, and the separation column is 5Å molecular sieve.

5 Photocatalytic H_2 production coupled MB purification

The photocatalytic H_2 production coupled with MB purification was carried out to elucidate the role of ·OH under the assistance of NaOH solutions (1 M). This process is analogous to the photocatalytic H_2 evolution experiment, with the exception of adding MB at a concentration of 30 mg L^{-1}. Prior to light irradiation, the solution was stirred in the dark to achieve adsorption equilibrium. Subsequently, 3 mL solution was withdrawn every 10 min and analyzed using a UV-Vis spectrophotometer at 664 nm to monitor the concentration of MB.

6 Hydroxyl free radical (·OH) detection

Using terephthalic acid (TA) as a molecular probe, we performed qualitative detection of hydroxyl radical (·OH) content on the surface of samples exposed to light through fluorescence spectroscopy. The tendency of surface ·OH to react with TA leads to the formation of strongly fluorescent 2-hydroxyterephthalic acid (TA-OH). Consequently, it was observed that the photoluminescence (PL) intensity of the reaction solution is directly proportional to the concentration of TA-OH produced in solution. In other words, under identical conditions, the fluorescence intensity exhibited by the reaction solution positively correlates with the quantity of ·OH generated during light exposure. This principle serves as a foundation for qualitatively assessing ·OH content.

The experimental procedure is as follows: The prepared catalyst was dispersed in a mixed solution containing a certain amount of TA and varying concentrations of NaOH. Under continuous stirring, the mixture was irradiated with a 300 W Xe-lamp. After 3 hours of reaction, a sample of the reaction solution was taken and filtered. Then, the hydroxyl radical signal was detected by PL spectroscopy with an excitation wavelength of 315 nm and an emission wavelength of 425 nm.

7 ECSA testing details

ECSA of the catalyst is usually estimated from the electrochemical double-layer capacitance (C_{dl}) of the catalytic surface. It can usually be calculated by the following Eq. (1). (C_s is the specific capacitance of the corresponding surface smooth samples, usually adopting 60 μF cm^{-2}.)

$$\text{ECSA} = C_{dl}/C_s \qquad (1)$$

Furthermore, the electrochemical double-layer capacitance can be firstly obtained by measuring the cyclic voltammetry (CV) curves at the different scan rates to obtain the corresponding non-Faraday double-layer capacitance current and then calculated by linear fitting. In the experiment, in order to obtain the electrochemical double-layer capacitance in the non-Faraday interval, the CV test should be carried out in the interval with no REDOX reaction occurring, which is in order to reflect the characteristics of the sample itself. Using open-circuit voltage as the central potential, we measure a series of curves with different scan rates under a certain potential range. For this system, the potential test range is from 0.2 to 0.4 V *vs.* SCE, and the scan rate is from 20 to 140 mV/s. Then, according to the current density at the center potential of each CV curve and the corresponding scanning rate to plot and fit the line. The slope of this line curve is C_{dl}.

The specific principle is as follows: non-Faraday current (i_c) is defined as following Eq. (2).

$$i_c = \frac{dq}{dt} = \frac{d(C_{dl}\varphi)}{dt} = C_{dl}\frac{d(\varphi)}{dt} + \varphi\frac{dC_{dl}}{dt} \qquad (2)$$

For the second term in Eq. (2), C_{dl} generally varies with the electrode surface state. When the scan range of potential is relatively small, the charged state of the electrochemical double-layer can be approximately considered to remain unchanged, and so does the corresponding C_{dl}. Hence, the second term in Eq. (2) can be ignored. In addition, due to the scanning speed of the linear scan being constant, the first term in Eq. (2) is a constant value. Therefore, Eq. (2) can be rewritten as following Eq. (3).

$$i_c = C_{dl}\frac{d(\varphi)}{dt} = \text{const} \quad (3)$$

From Eq. (3), it can be seen that $i_c \propto v$, where v is the scan rate of potential.

In summary, the slope of the fitting curve is C_{dl}, thus further estimating the ECSA of the catalyst based on Eq. (1).

8 Active radical capture experiment

The presence of $\cdot O_2^-$ was detected by the method of nitroimidazole chloride blue (NBT) conversion. NBT had a strong absorption peak at 260 nm of the UV absorption peak. $\cdot O_2^-$ could react with NBT, and the formation of methylation precipitate reduced the intensity of the UV absorption peak of NBT. The specific steps are as follows: 8 mg NBT was dissolved in 400 mL water and stirred evenly to form a yellow transparent solution. Then 5 mg of catalyst was dispersed in 100 mL of the above solution and stirred in the dark for 30 min to achieve adsorption desorption equilibrium. Finally, light it under a 300 W Xe-lamp. Use a syringe to take 4 mL of liquid every 5 min. After filtering, test it with a UV-visible spectrophotometer.

9 Density functional theory (DFT) study

All of the first principle calculations were based on the Vienna Ab initio Simulation Package (VASP). The interaction between ions and valence electrons was described by Projected Augmented Wave (PAW), and the exchange-correlation interaction was described by the Perdew-Burke-Ernzerhof generalized gradient approximation (PBE-GGA). The cut-off energy was set as 500 eV, and the convergence criteria for self-consistent electronic energy and residual force were respectively assumed to be 10-5 eV/atom and 0.02 eV/Å, which could ensure sufficient accuracy. A 6×6 slab with 144 atoms is employed to model the hexagonal phase $CdMnS_2$ (CMS) (002) surface. A vacuum region of with a 35 Å vacuum layer was added between periodic slabs. The k points are

set 1 × 1 × 1 based on Monkhorst-Pack meshes for all structures. To obtain accurate electron structures, convergence criteria were tightened, with electronic self-consistent field cycles considered convergent when the energy change was less than 1×10^{-6} eV. The results of the density of states (DOS) and charge density difference (CDD) were obtained by using the VASPKIT. A 2×1 slab with 68 atoms is employed to model $NiMoO_4$ (110) surface for comparison with the work function magnitudes of $CdMnS_2$ (002). The work function (Φ), defined as the energy required to remove an electron from the surface of a condensed solid into the external vacuum.

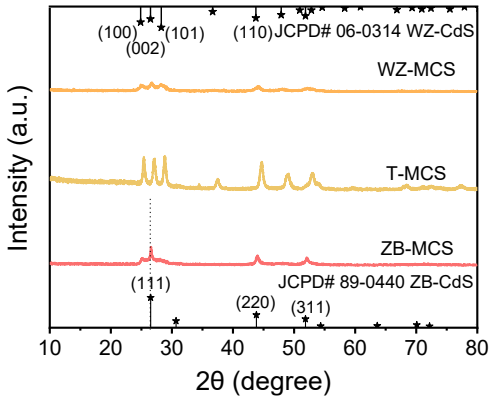

Fig. S1 XRD spectra of WZ-MCS, T-MCS and ZB-MCS

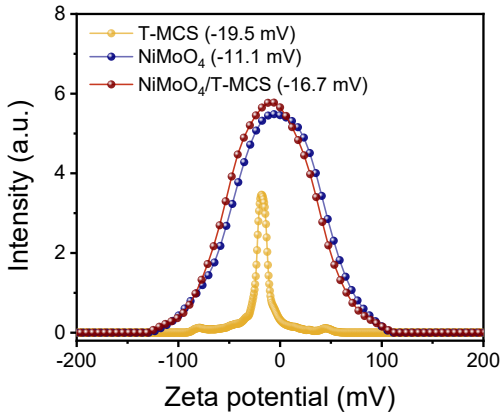

Fig. S2 Zeta potential of T-MCS and $NiMoO_4$ 6% $NiMoO_4$/T-MCS

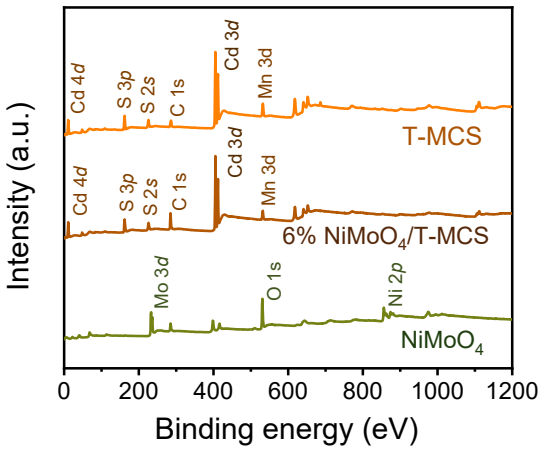

Fig. S3 XPS survey spectrum of T-MCS and $NiMoO_4$ 6% $NiMoO_4$/T-MCS

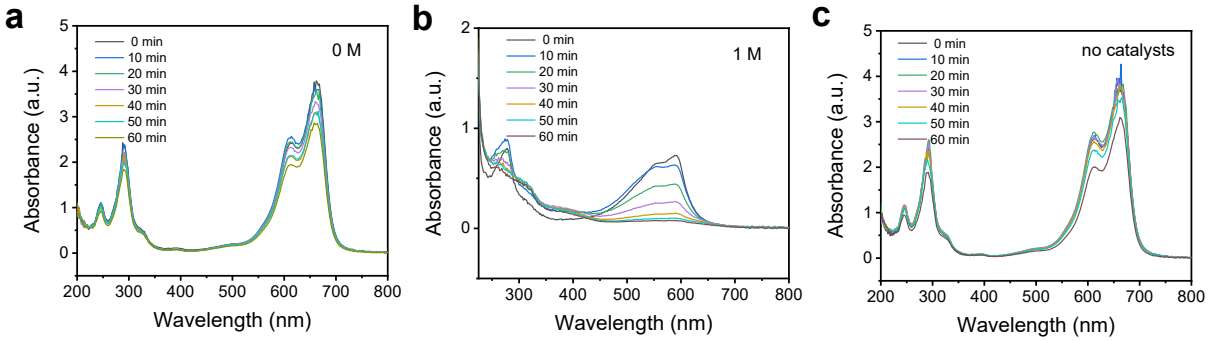

Fig. S4 (a-c) Raw data for MB degradation over 6% $NiMoO_4$/T-MCS

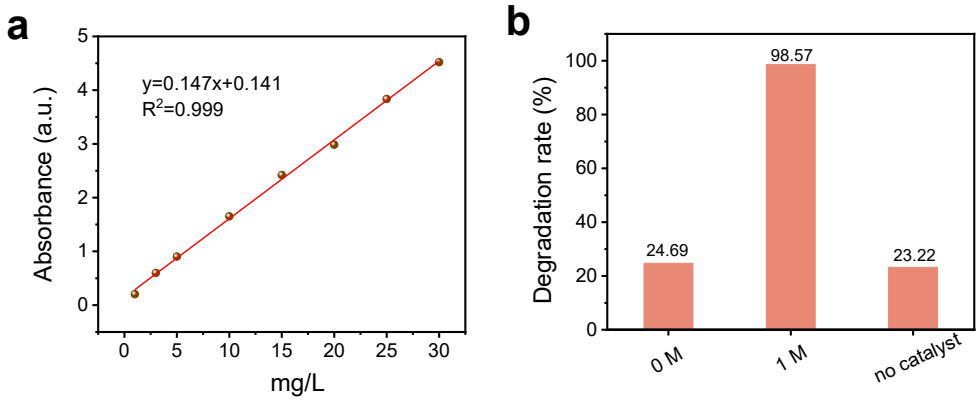

Fig. S5 (a) The standard curve of MB and (b) degradation rate of each sample at 40 min

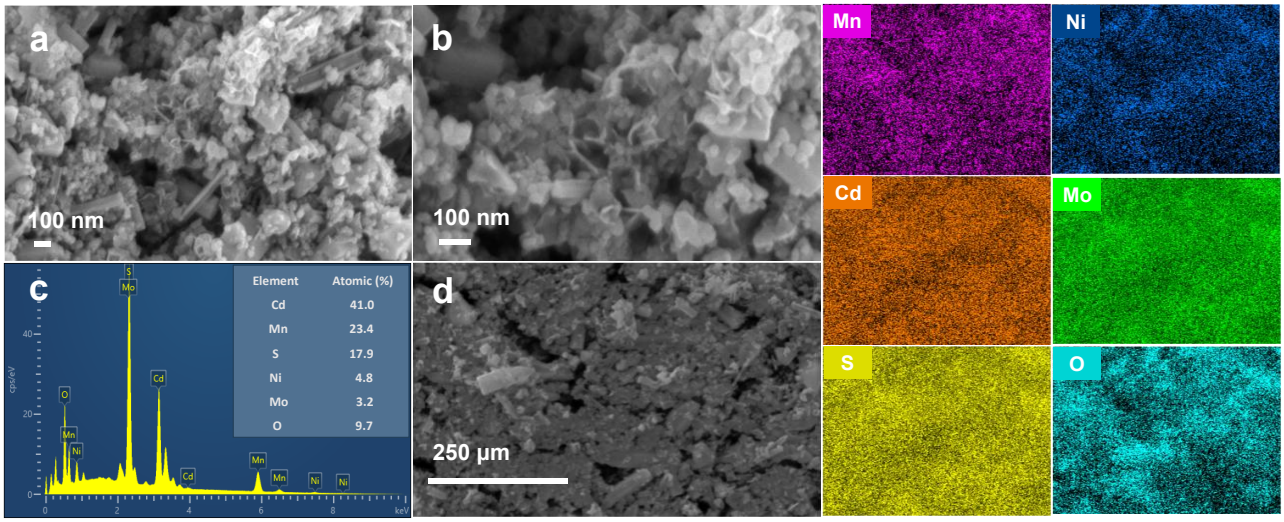

Fig. S6 (a-b) SEM, (c) EDS spectrum and (d) elemental mapping of 6% $NiMoO_4$/T-MCS-1M

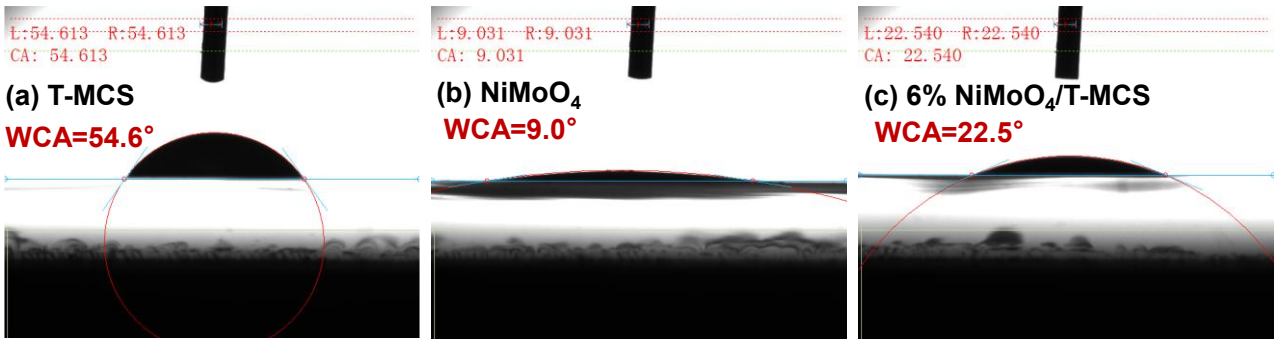

Fig. S7 Water contact angle test (a) T-MCS, (b) $NiMoO_4$ and (c) 6% $NiMoO_4$/T-MCS

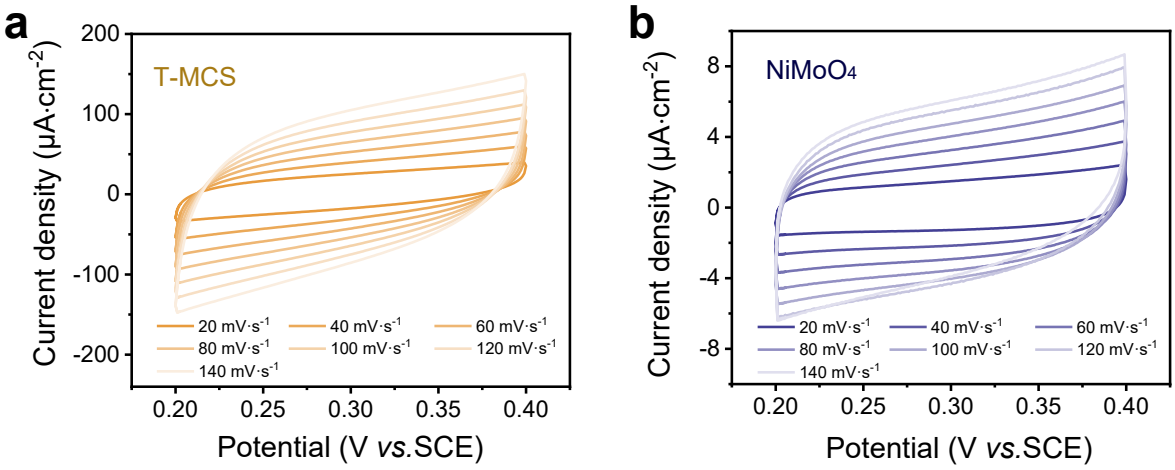

Fig. S8 CV curves at different scan rates of (a) T-MCS and (b) $NiMoO_4$

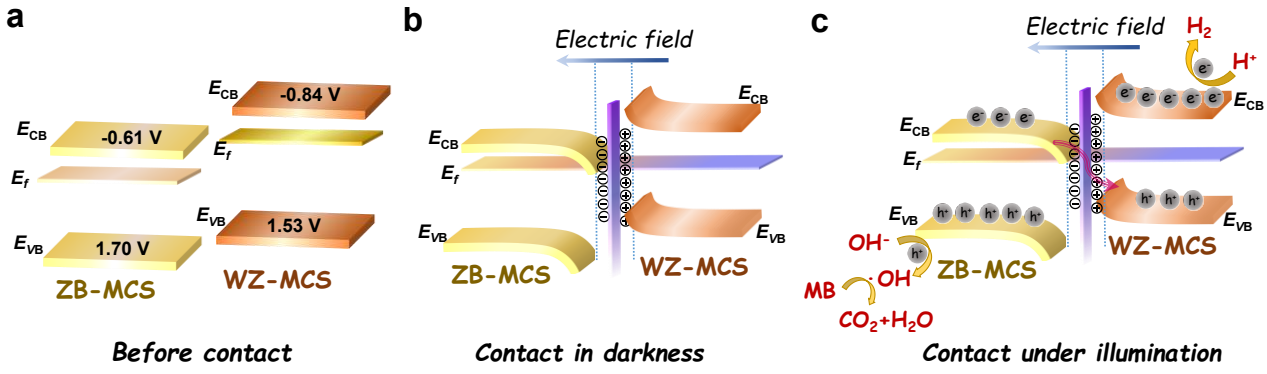

Fig. S9 Charges transfer mechanism over T-MCS under illumination